

© 2020. A. Lejzerowicz, M. Wutke.

This is an open-access article distributed under the terms of the Creative Commons Attribution-NonCommercial-NoDerivatives License (CC BY-NC-ND 4.0, <https://creativecommons.org/licenses/by-nc-nd/4.0/>), which permits use, distribution, and reproduction in any medium, provided that the Article is properly cited, the use is non-commercial, and no modifications or adaptations are made.



GPR AS A SUPPORT TOOL IN DETERMINING THE CAUSES OF FAILURE OF OBJECTS BUILT IN THE “WHITE BOX” TECHNOLOGY

A. LEJZEROWICZ¹, M. WUTKE²

From the construction made in the “white box” technology, first of all tightness is required - on the structural elements there should not be any cracks or scratches, through which water could penetrate, which in consequence may lead to deformation of structural elements and even losing of their load-bearing capacity. Among the methods enabling the location of weakened places in watertight concrete, the ground penetrating radar (GPR) method is effective because the local occurrence of water in the structure evokes a clear and unambiguous anomaly on the radargram. In addition, the GPR method allows you to indicate places where water flows without the necessity of excluding the object from use and interference in the construction layers. The designation of such locations will make it possible to undertake technical activities that can facilitate the takeover of water and thus ensure the desired load-bearing capacity and usability of the object. Using the GPR method, you can also designate places that have already been deformed – discontinuities or breaking. The article presents a case study of investigations that determine the causes of leakage of tunnels made in the “white box” technology in: twice within the bottom slab of the tunnel (1 GHz air-coupled and 400 MHz ground-coupled antenna) and once in the case of tunnel walls (1.6 GHz ground-coupled antenna).

Keywords: non-destructive testing methods, ground penetrating radar (GPR), “white box” technology, dielectric constant, GPR wave amplitude

¹ PhD, Warsaw University of Technology, Faculty of Civil Engineering, Al. Armii Ludowej 16, 00-637 Warsaw, Poland, e-mail: a.lejzerowicz@il.pw.edu.pl

² DSc, Eng, TPA Sp. z o.o., ul. Parzniewska 8, 05-800 Pruszków, Poland, e-mail: malgorzata.wutke@tpaqi.com

1. INTRODUCTION

The "white box" technology is based on a complete construction, material and technology system, which replaces coating solutions in the form of heavy anti-water and anti-moisture insulations made of bituminous and mineral materials ("black box"), instead using a special concrete property: water tightness [1]. In this case, the construction itself is made of watertight concrete. In order to obtain a "white box", it is necessary to meet and co-operate several basic elements of this technology, which includes system sealing accessories, appropriate reinforcement of structures, concreting divided into working plots, proper care of concrete.

The basic assumption of the "white box" technology is the use of waterproof concrete together with sealing elements and accessories [1]. Concrete that is used to make the "white box" construction has two functions: construction and waterproofing. The structural function is related to meeting the requirements of the appropriate, designed compression strength class, but equally important - durability during operation. The concrete waterproofing function is to provide an effective barrier for groundwater or other water that acts on the structure. The construction performed in the "white box" technology requires above all tightness and a long service life. Therefore, already at the stage of designing of concrete in the "white box" technology specific requirements should be provided for the properties of concrete and technology of performance, otherwise it may lead to leaks [2-4]. Concrete contraction may contribute to leakage, including plastic shrinkage associated with improper water care. It is also important to prevent (through proper thermal care) the occurrence of variable thermal and humidity fields, which can lead to scratches of the structure. The critical spots of potential leaks are dilatation between the segments forming the object, places where there are working intervals in concreting, places where the structure passes through the installation elements of the object. On the other hand, elements of too large dimensions between dilatation are exposed to scratching [1].

Because of design and implementation errors as well as unsuitable materials used for construction, structural damage may occur, which in the presence of water will lead to leaks (Fig.1) [3]. Leaks in the next phase lead to the break of construction continuity, which can affect the loss of load-bearing capacity and safety of use of the object (Fig. 2).

One of the methods enabling the non-destructive location of leakages and the location of deformations in the cross-section without the necessity of excluding the object from use is the ground penetrating radar method [5-7]. Effective detection of this type of places allows for taking

corrective actions that will allow sealing and removing water, possibly repairing the deformation already created, and thus maintaining the designed load-bearing capacity and usability of the facility.

The article presents examples of practical use of the GPR method to locate leaks and damages in the bottom slab and tunnel walls made in the "white box" technology. The presented examples confirm the usefulness of the GPR method for the non-destructive detection of leakages and deformations as well as the determination of their range and location in objects made in the "white box" technology.



(a)



(b)



(c)



(d)

Figure 1. Leaks in tunnel built in the 'white box' technology: (a) Leakage on the whole wall of the tunnel; (b) Leak at the dilation and in the vicinity of the working gap; (c) Efflorescence and leakage in the area of wall dilatation; (d) Outflow of water under pressure after drilling the control well.

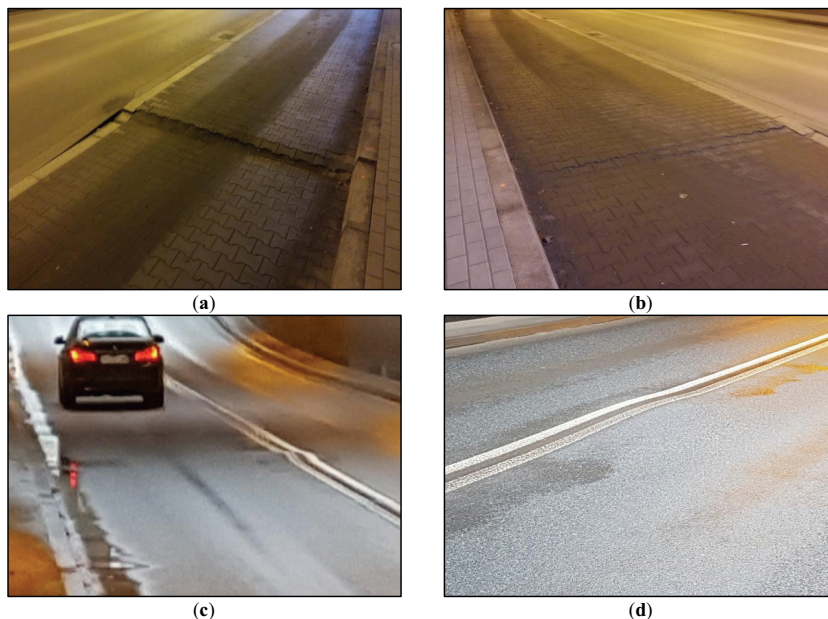


Figure 2. Structural damage resulting from leaks in tunnels: (a) and (b) cracking and elevation of the pedestrian walkway in the tunnel; (c) and (d) deformation in the form of elevation of asphalt layers of the tunnel.

2. MATERIALS AND METHODS

2.1. GROUND PENETRATING RADAR METHOD

During this study a ground penetrating radar (GPR) investigations were carried out. It is a very-high-frequency electromagnetic technique used to produce high-resolution images. During GPR surveys, a transmitting antenna is sending a pulse of high-frequency electromagnetic waves of known frequency into the ground. Then an electromagnetic wave penetrates the medium where it may undergo transmission, reflection and/or refraction (resulting from a change in electrical parameter). In recorded images (radargrams), the electromagnetic waves that were reflected from the boundaries between deposits characterized by different values of their dielectric constant ϵ_r are analyzed [8-13]. The 'quality' (reflection strength, amplitude) recorded on radargrams and the depth range depends on the contrast of the electrical properties between the two media [14-16]. Deposits

or materials with a high dielectric constant can be distinguished based on the attenuation of the electromagnetic wave. Because water has the highest dielectric constant ($\epsilon_r = 81$) and a high conductivity, the water content adversely affects signal propagation – it increases the energy and it is reducing the depth range of GPR prospecting [14, 17, 18]. For all GPR profiles only basic processing was done including time-depth conversion, background removal, exponential signal amplification and vertical filtering using the Savitzky-Golay method.

2.2. INVESTIGATIONS OF THE BOTTOM SLAB OF THE TUNNEL WITH DEFORMATION IN THE FORM OF ELEVATION OF THE ASPHALT SURFACE - MEASUREMENTS AND INTERPRETATION PROCEDURE

For the measurements of the bottom slab of the tunnel, where deformation in the form of elevation of the asphalt pavement was observed, a GSSI radar system with a 1.0 GHz air-coupled antenna was used (detection range - about 90-150 cm for dry concrete and 70-90 cm for saturated concrete). Measurements were taken along the tunnel in parallel profiles (spacing: 90 cm) to cover the whole tunnel surface of the studied area (Fig. 3). Parallel profiles were also used to prepare maps presenting the frequency spectrum of the waves propagated through the medium after Short Time Fourier Transform (STFT) in the time window 2 – 3 ns.

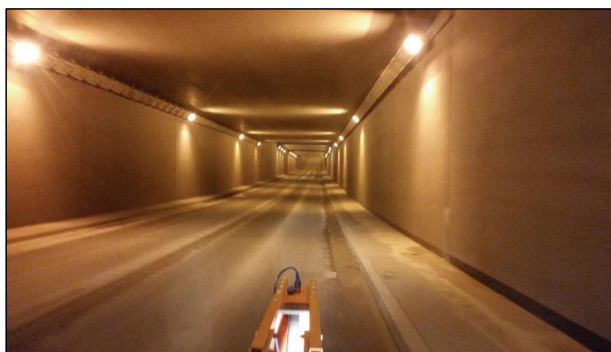


Figure 3. Measurements made on the bottom slab of the tunnel with 1.0 GHz air-coupled antenna.

The analysis of the amplitudes of electromagnetic waves, of dielectric constants on the surface of the tunnel's roadway and of the frequency spectrum of the wave at the depth between the asphalt layers and the bottom slab were carried out. The frequency of the electromagnetic wave was analyzed at the depth corresponding to the boundary of asphalt layers and bottom slab.

Additionally, the values of dielectric constants of the wearing course of the tunnel surface were analyzed.

2.3. INVESTIGATIONS ON THE BOTTOM SLAB OF THE TUNNEL WITH DEFORMATION IN THE FORM OF CRACKING OF THE PEDESTRIANS WALKWAY

The GSSI radar systems with 400 MHz ground-coupled antenna (penetration range - about 2.4-4 m for a dry, homogeneous medium and 1.7-2.4 m for saturated concrete) and a 1.0 GHz air-coupled antenna were used for the measurements being the subject of this study. The measurements were taken with each antenna in 5 lines along the tunnel to cover the whole tunnel surface (Fig. 4).



Figure 4. Measurements of the bottom slab of the tunnel with 1.0 GHz air-coupled antenna and 400 MHz ground-coupled antenna. To conduct investigations with two antennas at the same time, a special trolley was prepared.

2.4. INVESTIGATIONS OF A TUNNEL WALL

The IDS GPR system with a 1.6 GHz ground-coupled antenna was used to measure the dilatation of the tunnel wall (detection range - about 60-90 cm for a dry, homogeneous medium and 40-60 cm for saturated concrete). Measurements were made along each wall dilatation in three passes: on the left and right side of the dilatation and directly on the dilatation (Fig. 5).

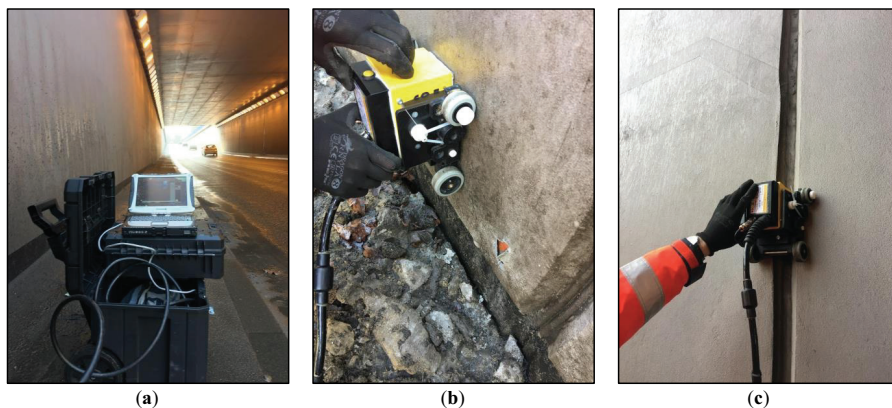


Figure 5. Measurements of dilatation of tunnels wall with a 1.6 GHz ground-coupled antenna.

3. RESULTS AND DISCUSSION

3.1. THE RESULTS OF THE INVESTIGATIONS OF THE BOTTOM SLAB OF THE TUNNEL WITH DEFORMATION IN THE FORM OF ELEVATION OF THE ASPHALT SURFACE

Fig. 6 presents radargrams from measurements of the section covering the observed deformation of the surface. The blue, continuous line indicates the border between the asphalt layers and the bottom slab (at a depth of 11.5 cm). The results of measurements from passage no. 2, 3 and 4 indicate the presence of water between the asphalt layers and the bottom slab: places with a high value of the wave reflection amplitude due to the presence of water are marked with a red rectangle. High amplitude values in the area of the observed surface bulge confirm the presence of moisture (in Fig. 7 it is marked with a red rectangle). Similar anomalies are not observed for the rest of the object's bottom slab. In Fig. 7 it is shown that moisture between the asphalt layers and the bottom slab of the tunnel causes an increase of high frequencies in the spectrum of the wave propagating through the structure (here in the range of 2000 – 5000 MHz) after Short Time Fourier Transform in the time window corresponding to the border between the asphalt layers and the concrete part of the object. Changes in the EM wave spectrum propagating in a medium containing water are determined by two mechanisms: absorption and reflection. The water in the medium absorbs the high-frequency wave components more strongly, which results from the nature of the imaginary dependence of the dielectric constant on frequency; the central frequency is therefore shifted towards smaller values. On the other hand, the same relationship

between the real and imaginary dielectric constant components causes the opposite effect when the EM pulse is reflected from the water surface (e.g. a water lens or a highly hydrated area). The reflection coefficient increases with the wave frequency when the real component is fairly constant and the imaginary component increases. Therefore, stronger reflexes in the higher frequency range lead to a shift of the central frequency in the received wave spectrum towards higher values.

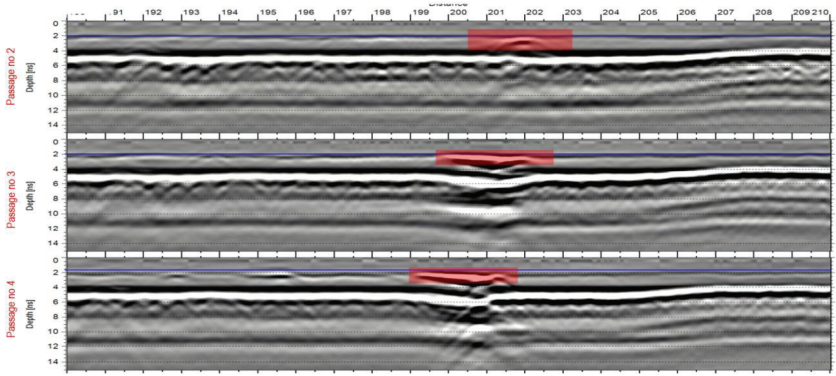


Figure 6. Test results of the bottom to

m slab - high amplitude values under the asphalt indicate the presence of water in this place (after [19], modified). Hyperbolas: reinforcement of the first layer of the tunnel bottom slab (bars perpendicular to the scan direction).

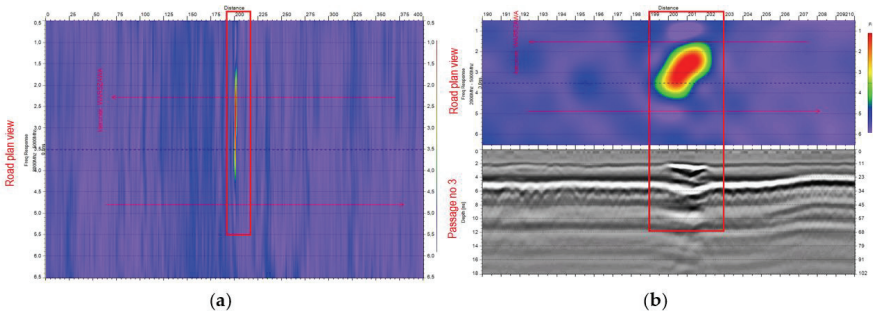


Figure 7. Investigations results of the bottom slab of the tunnel - maps of frequency spectrum of the wave propagated through the structure in the time window 2 – 3 ns corresponding to the depth between the asphalt layers and the bottom slab of the tunnel: (a) shows that similarly high amplitudes are not observed in the rest of the tunnel; (b) the map was compared to the same radargram. High amplitude values on the maps are marked with a red rectangle (after [19], modified).

In Figure 8, a blue rectangle indicates increased values of dielectric constants: in the middle of the road resulting from the presence of road salt (chlorides); at the lower edge of the road (at the bottom of the drawing) resulting from incorrect water drainage through drainage wells to the drainage system; at the higher edge of the road resulting from migration of water from dilatation to the tunnel surface. The deformation area of the asphalt surface is marked with a red rectangle - higher values of dielectric constants indicate that the residual water is pushed to the surface, most likely as a result of vehicle traffic. The area of deformation is characterized by higher values of dielectric constants (blue rectangle in Fig. 8) from the values characteristic for the surface of the mineral-asphalt mix (MAM) in the dry state - this means that MAM free spaces are filled with water. Such a result may indicate a damage to the insulation between MAM and the concrete slab and the outflow of water remaining under the insulation through the asphalt layers.

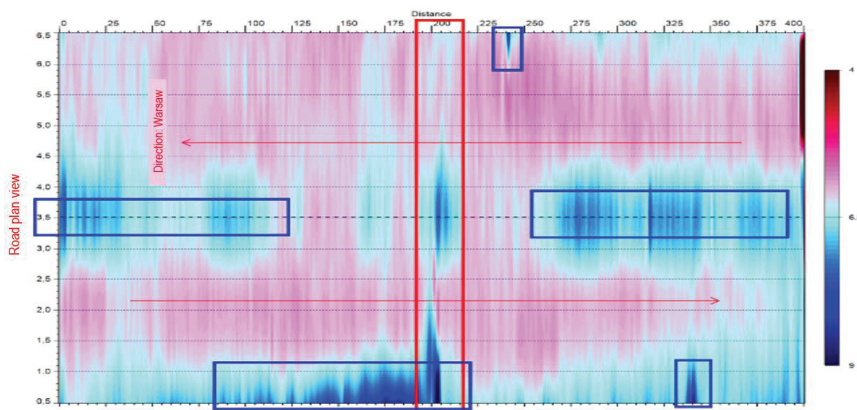


Figure 8. Maps of dielectric constants on the pavement surface (after [19], modified).

3.2. INVESTIGATIONS RESULTS OF THE BOTTOM SLAB OF THE TUNNEL WITH CRACKING AND ELEVATION OF THE PEDESTRIAN WALKWAY IN THE TUNNEL

Figure 9 presents radargrams performed using 1.0 GHz air-coupled antenna. Profiles 1-3 are made on the roadway, where the layer system is a 24 cm bundle of asphalt layers on the aggregate (total thickness: about 64 cm). Under the road surface there is a reinforced concrete coat (at least 20 cm) on the bottom slab, separated from the bottom slab by waterproofing. The yellow, continuous line

indicates the boundaries between the asphalt layers and the aggregate. The red, dotted line indicates probable voids created as a result of elevating the asphalt layers and detaching them in this way from the aggregate in the area of dilatation between neighboring segments of the structure. The boundary between the aggregate and the protective cover of the bottom slab is beyond the reach of used antenna. Profile 4 was made in the bus bay. Layer system there is a pavement cube on the cement-sand bedding (13 cm in total) laid on a reinforced concrete protective cover with a minimum thickness of 67 cm. The red, dashed line indicates an offset of pavement cubes (between segments) and a vertical shift of the protective cover with respect to adjacent segments.

The bottom of the protective cover is beyond the reach of the 1.0 GHz antenna. Profile 5 was made on the platform of the bus stop. Layer system is there about 100-cm thick road surface of which the top layer is a concrete cube on the cement-sand bedding. The yellow, continuous line indicates the border between the concrete cube and the foundation of the cement stabilized aggregate. The boundary between the aggregate and the protective cover of the bottom slab is beyond the reach of used antenna.

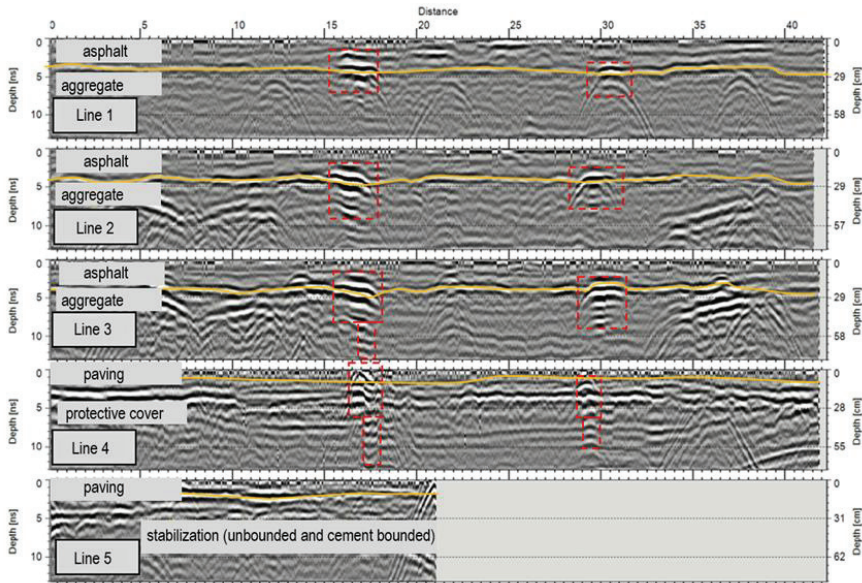


Figure 9. Investigation results of the bottom slab of the tunnel with deformation in the form of cracking and elevation of the pedestrian walkway - GPR profiles recorded with a 1.0 GHz antenna. Hyperbolas appear in the aggregate layer, those are probably drain pipes.

Figure 10 presents radargrams from investigations using 400 MHz antenna - the range of this antenna for the studied medium is about 300 cm, therefore following analysis concerns a depth of up to 300 cm. Profiles 1-3 were made on the roadway, where the layer system is a 24-cm bundle of asphalt layers on the aggregate (a total of about 64 cm). Under the road surface is a reinforced concrete coat (at least 20 cm) on an 80-cm bottom slab, separated from it by waterproofing. The red, dotted line indicates probable voids created as a result of elevating the asphalt layers detaching them in this way from the crushed stones layer. A purple, continuous line is marking a fault location between neighboring structure segments at the depth of the protective cover. The underside of the bottom slab is marked with a yellow, continuous line. It is noted that strengthening and weakening of the amplitude of the horizontal reflex corresponding to the underside of the bottom slab are noticeable, although it cannot be unequivocally determined whether those are changes resulting from damage of the bottom slab.

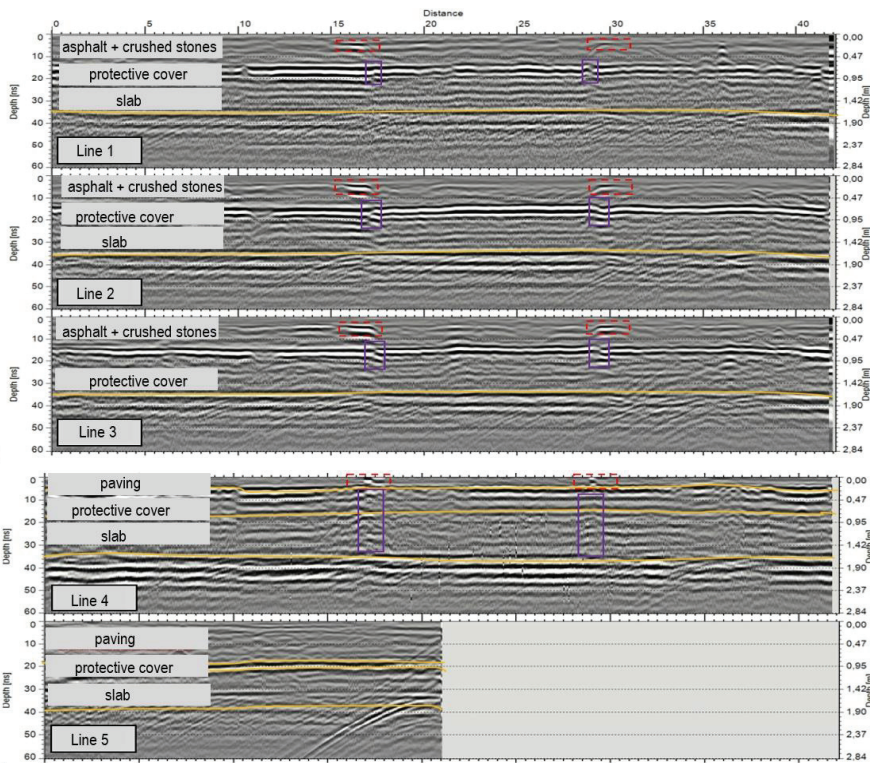


Figure 10. Investigations results of the bottom slab of the tunnel with deformation in the form of a pedestrian walkway cracking - GPR profiles (line 1-5) recorded with a 400 MHz antenna.

Profile 4 was made in the bus bay. Layer system there is a pavement cube on the cement-sand bedding (13 cm in total) laid on a reinforced concrete protective cover with a minimum thickness of 67 cm. A line of pavement cubes is marked with a red, dotted line. The purple, continuous line shows anomalies in the area of dilatation between the construction segments at the depth of the protective cover and the bottom slab. While in the case of a protective coat, the vertical shift of the protective coat is observed in relation to the neighboring segments coats and elevating it up, in the case of the bottom slab the interpretation of the anomaly is not unambiguous.

Profile 5 was made on the platform of the bus stop. Layer system in this place is as follows: about 100-cm road surface, underneath there is a 15-cm layer of protective coat and 80-cm thick bottom slab, separated by waterproofing. The yellow, continuous line indicates the boundaries between the road surface and the protective coat, protective coat and bottom slab, and the underside of the bottom slab. On profile 5, no significant anomalies are observed in the area of the protective coat and the bottom slab.

3.3. THE INVESTIGATION RESULTS OF TUNNEL WALLS

Figure 11 shows radargrams from measurements in the area of the dilatation from the deformation area observed on the surface. On radargrams made on both sides of the dilatation, diffraction hyperbola corresponding to steel bars (reinforcement) in the structure are visible. Reinforcement (due to the fact that it reflects electromagnetic waves) makes it impossible to determine the moisture status of the wall in this place. Anomalies on a radargram from passing directly above the gap may indicate moisture. However, it should be remembered that the presence of reinforcement in the close distance to the gap affects the GPR measurement result and the interpretation of measurements of reinforced elements directed to determine the humidity status is often ambiguous.

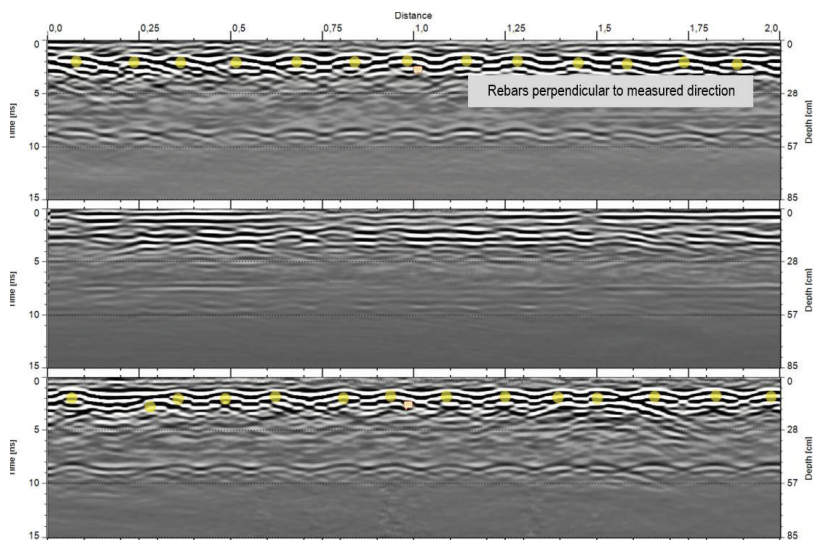


Figure 11. The results of GPR investigations of tunnel walls.

3. CONCLUSIONS

The concept of "white box" as a water protection system is gaining more and more popularity. Technological and execution errors lead to leaks leading to premature degradation of the reinforced concrete. Effective detection of this type of places allows to take corrective actions that will allow sealing and removal of water, thus ensuring the designed load-bearing capacity and usability of the facility. One of the methods enabling non-destructive location of leak points without having to switch off the facility from use is the ground penetrating radar method.

Based on GPR investigations of the bottom slab with deformation of the asphalt surface of the tunnel, it was stated that:

- water was occurring in the area of observed deformation of the tunnel surface, between asphalt layers and bottom slab;
- no similar anomalies were occurring in the rest of the tunnel;
- there is a possible damage to the insulation between the asphalt layers and the bottom slab, and water movement from the deformation area upwards due to the movement of trucks

causing an increase in the water pressure inside the deformation (this would explain the gradual decrease of deformation);

- there is a possible water retention in the area of drainage wells;
- migration of water is possible, from dilatation to the asphalt surface of the tunnel.

Based on GPR investigations of the bottom slab with the deformation of the pedestrian walkway with the 1.0 GHz air-coupled antenna, it was found that:

- voids created as a result of lifting the asphalt layers upwards and detaching them from the aggregate are occurring;
- there is an elevation of the pavement construction segment.

Based on GPR investigations of the bottom slab with pedestrian pavement deformation using 400 MHz ground-coupled antenna, it was stated that there is:

- the visibility of places with a clear lack of continuity of the protective structure of the bottom slab - on this basis, it can be assumed that water has raised one of the segments of the bottom slab's protective cover, elevating the layers above the shell structure. While in the case of a protective coat, it is possible to assume elevation of the segment upwards, while in the case of a bottom slab the interpretation of the anomaly is not unambiguous. GPR investigations below the level on which the reinforcing mesh is located (strongly scattering radar signal) does not allow unambiguous determination of the structure.

Based on GPR research of selected dilatation of tunnel walls:

- moistening of all joints indicated for testing was found;
- due to the reinforcement concentration, it was not possible to confirm the existence of internal waterproofing tape.

The case study presented in the article confirms the usefulness of the GPR method for the non-destructive detection of leakages and resulting from them structural deformations of structures made in the "white box" technology.

Funding: This research did not receive any specific grant from funding agencies in the public, commercial, or not-for-profit sectors. The article was written thanks to the agreement between the TPA Sp. z o. o. research laboratory and a Faculty of Civil Engineering, Warsaw University of Technology on cooperation in the field of research, education and human resources.

REFERENCES

1. Bajorek G., Kiernia-Hnat M., Świerczyński W. Biała wanna – technologia szczelnej konstrukcji. *Budownictwo, Technologie, Architektura* 2015, 2: 72-74, 2015. (in Polish)
2. Czarnecki L., Łukowski P., Garbacz A. Naprawa i ochrona konstrukcji z betonu. *Komentarz do PN-EN 1504*, PWN, Warszawa, pp. 271, 2017. (in Polish)
3. W. Jackiewicz-Rek W., M. Konopska-Piechurska M., Załęgowski K., Garbacz A. Specyfika napraw uszkodzeń nawierzchni betonowych. *Materiały Konferencji Naukowo-Technicznej Awarie Budowlane, Szczecin-Międzyzdroje*, pp. 779-790, 2015. (Conference Proceedings, in Polish)
4. Kłos K., Jackiewicz-Rek W. Czynniki kształtujące szczelność betonu w technologii „białej wanny”. *Materiały Budowlane* 549: 46-48, 2018. (in Polish)
5. Hoła K., Bień J., Sadowski L., Schabowicz K. Non-destructive and semi-destructive diagnostics of concrete structures in assessment of their durability. *Bulletin of the Polish Academy of Sciences, Technical Sciences* 63 (1): 87-96, 2015.
6. Garbacz A., Harassek P., Van der Wielen A., Piotrowski T., Courard L., Nguyen F. Diagnostyka konstrukcji betonowych za pomocą impact-echo i radaru. *Materiały Konferencji „Dni Betonu”*, Wisła, pp. 977-985, 2010. (Conference Proceedings in Polish)
7. Wutke M., Konopska-Piechurska M., Jackiewicz-Rek W., Załęgowski K., Garbacz A. Zastosowanie GPR przy ocenie stopnia zawilgożenia elementów posadowienia w prognozowaniu trwałości betonu w parkingu podziemnym. *Materiały Konferencji Naukowo-Technicznej „Awarie Budowlane 2017”*, Szczecin-Międzyzdroje, pp. 951-961, 2017. (Conference Proceedings, in Polish)
8. Neal A. Ground-penetrating radar and its use in sedimentology: principles, problems and progress. *Earth-Science Review* 66: 261-330, 2004.
9. Jol H.M. *Ground Penetrating Radar: Theory and Applications*, Elsevier, pp. 544, 2009.
10. Daniels D.J. *Ground penetrating radar*, 2nd edition. The Institution of Electrical Engineers, London, pp. 734, 2004.
11. Eyuboglu S., Mahdi H., Al-Shukri H. Detection of water leaks using Ground Penetrating Radar; University of Arkansas at Little Rock, pp. 18, 2004.
12. Balaysac J.P. Determination of volumetric water content of concrete using Ground-Penetrating Radar, *Cement and Concrete Research* 37(8): 164-1171, 2007.
13. Wutke M. Use of EM waves (radar measurement) combined to resistivity measurement for characterization of the concrete. Master Thesis, Politechnika Wrocławska, Wrocław, 2015.
14. Wutke M., Lejzerowicz A., Jackiewicz-Rek W., Garbacz A. Influence of variability of water content in different states on electromagnetic waves parameters affecting accuracy of GPR measurements of asphalt and concrete pavements. *MATEC Web of Conferences* 262: 1–6, 2019.
15. Lejzerowicz A., Kowalczyk S. Usefulness of GPR surveys for identification of internal features of Vistula River deposits in Natura 2000 areas. *Prace i Studia Geograficzne* 63.2: 7-20, 2018 (in Polish with English summary).
16. Lejzerowicz A. Internal architecture of fluvial deposits and the morphology of the selected sections of Narew River valley in Warsaw area (central Poland) based on GPR investigations. In: *17th International Conference on Ground Penetrating Radar (GPR2018)*. IEEE Xplore Digital Library, pp. 348–353, 2018.
17. Lejzerowicz A., Kowalczyk S., Wysocka A. The usefulness of ground-penetrating radar images for the research of a large sand-bed braided river: case study from the Vistula River (central Poland). *Geologos* 20(1): 35–47, 2014.
18. Benedetto A., Pajewski L. *Civil Engineering applications of Ground Penetrating Radar*, Springer, Switzerland, pp. 147-194, 2015.
19. Wutke M., Lejzerowicz A., Jackiewicz-Rek W., Garbacz A. Application of the ground penetrating radar method to leak detection of objects made in the "white box" technology: a case study. Conference “Dni Betonu”, Wisła, Poland; 2018 (in Polish with English summary).

LIST OF FIGURES AND TABLES:

Fig. 1. Leaks in tunnel built in the 'white box' technology: (a) Leakage on the whole wall of the tunnel; (b) Leak at the dilation and in the vicinity of the working gap; (c) Efflorescence and leakage in the area of wall dilatation; (d) Outflow of water under pressure after drilling the control well.

Rys. 1. Przecieki w tunelu zbudowanym w technologii "białej wanny": a) Wyciek na całej ścianie tunelu; b) wyciek przy dylatacji i w pobliżu szczeliny roboczej; c) wykwyty i nieszczelności w obszarze dylatacji ścian; d) Odpływ wody pod ciśnieniem po odwierceniu studni kontrolnej.

Fig. 2. Structural damage resulting from leaks in tunnels: (a) and (b) cracking and elevation of the pedestrian walkway in the tunnel; (c) and (d) deformation in the form of elevation of asphalt layers of the tunnel.

Rys. 2. Uszkodzenia konstrukcyjne wynikające z przecieków w tunelach: a) i b) pęknięcie i uniesienie chodnika dla pieszych w tunelu; c) i d) deformacja w postaci wyniesienia warstw asfaltu w tunelu

Fig. 3. Measurements made on the bottom slab of the tunnel with 1.0 GHz air-coupled antenna.

Rys. 3. Pomiary wykonane na płycie dennej tunelu z wykorzystaniem anteny o częstotliwości 1,0 GHz sprzężonej z powietrzem.

Fig. 4. Measurements of the bottom slab of the tunnel with 1.0 GHz air-coupled antenna and 400 MHz ground-coupled antenna. To conduct investigations with two antennas at the same time, a special trolley was prepared.

Rys. 4. Pomiary płyty dennej tunelu z wykorzystaniem anteny o częstotliwości 1,0 GHz sprzężonej z powietrzem i anteny o częstotliwości 400 MHz sprzężonej z ziemią. Przygotowano specjalny wózek, aby przeprowadzić jednoczesne badania dwoma antenami.

Fig. 5. Measurements of dilatation of tunnels wall with a 1.6 GHz ground-coupled antenna.

Rys. 5. Pomiary dylatacji ściany tunelu z wykorzystaniem anteny o częstotliwości 1,6 GHz sprzężonej z ziemią.

Fig. 6. Test results of the bottom slab - high amplitude values under the asphalt indicate the presence of water in this place (after [19], modified).

Rys. 6. Wyniki badań płyty dennej - wysokie wartości amplitud pod asfaltem wskazują na obecność wody w tym miejscu (za [19], zmienione).

Fig. 7. Investigations results of the bottom slab of the tunnel - maps of frequency spectrum of the wave propagated through the structure in the time window 2 – 3 ns corresponding to the depth between the asphalt layers and the bottom slab of the tunnel: (a) shows that similarly high amplitudes are not observed in the rest of the tunnel; (b) the map was compared to the same radargram. High amplitude values on the maps are marked with a red rectangle (after [19], modified).

Rys. 7. Wyniki badań płyty dennej tunelu - mapy widma częstotliwości fali propagującej przez strukturę w przedziale czasowym 2-3ns odpowiadające głębokościom między warstwami asfaltu a płytą denną tunelu: a) widać, że podobnie wysokie amplitudy nie są obserwowane w pozostałej części tunelu; b) mapa została

porównana z tym samym radargramem. Wysokie wartości amplitud na mapach są oznaczone czerwonym prostokątem (za [19], zmienione).

Fig. 8. Maps of dielectric constants on the pavement surface (after [19], modified).

Rys. 8. Mapy stałych dielektrycznych na powierzchni chodnika (za [19], zmienione).

Fig. 9. Investigation results of the bottom slab of the tunnel with deformation in the form of cracking and elevation of the pedestrian walkway - GPR profiles recorded with a 1.0 GHz antenna.

Rys. 9. Wyniki badań płyty dennej tunelu z deformacją w postaci pęknięcia i wyniesienia chodnika dla pieszych - profile GPR zarejestrowane za pomocą anteny 1.0 GHz.

Fig. 10. Investigations results of the bottom slab of the tunnel with deformation in the form of a pedestrian walkway cracking - GPR profiles recorded with a 400 MHz antenna.

Rys. 10. Wyniki badań płyty dennej tunelu z deformacją w postaci pęknięcia chodnika dla pieszych - profile GPR zarejestrowane za pomocą anteny 400 MHz.

Fig. 11. The results of GPR investigations of tunnel walls.

Rys. 11. Wyniki badań GPR ścian tuneli.

GPR JAKO NARZĘDZIE WSPIERAJĄCE W OKREŚLANIU PRZYCZYŃ AWARII OBIEKTÓW ZBUDOWANYCH W TECHNOLOGII "BIAŁEJ WANNY"

Słowa kluczowe: badania nieinwazyjne, metoda georadarowa (ang. *ground penetrating radar* - GPR), technologia "białej wanny", stała dielektryczna, amplituda fali elektromagnetycznej

Od konstrukcji wykonanej w technologii "białej wanny" wymagana jest przede wszystkim szczelność - na elementach konstrukcyjnych nie powinno być żadnych pęknięć ani zadrapań, przez które woda może przenikać, ponieważ to w konsekwencji może prowadzić do deformacji elementów konstrukcyjnych, a nawet utraty ich nośności. Wśród metod umożliwiających lokalizację osłabionych miejsc w wodoszczelnym betonie, metoda georadarowa (ang. *ground penetrating radar* - GPR), jest skuteczna, ponieważ lokalne występowanie wody w strukturze wywołuje wyraźną i jednoznaczną anomalię na otrzymanym obrazie (radargramie). Ponadto metoda GPR pozwala wskazać miejsca, w których woda przepływa bez konieczności wyłączenia obiektu z użytkowania i bez ingerowania w warstwy konstrukcyjne. Wyznaczenie takich miejsc umożliwia podjęcie działań technicznych, które mogą ułatwić przejście wody, a tym samym zapewnić pożądaną nośność i użyteczność obiektu. Za pomocą metody GPR można również wyznaczyć miejsca, które zostały już zdeformowane - miejsca nieciągłości lub ugięć czy spękań. Artykuł przedstawia studium przypadku oraz badania, które umożliwiły określenie przyczyny wycieku w obrębie tunelu wykonanego w technologii "białej wanny" - w obrębie płyty dennej tunelu (z wykorzystaniem anteny o częstotliwości 1 GHz sprzężonej z powietrzem oraz z wykorzystaniem anteny o częstotliwości 400 MHz sprzężonej z ziemią), jak również w przypadku ścian tunelu (antena o częstotliwości 1,6 GHz sprzężona z ziemią).

